JCTC Journal of Chemical Theory and Computation

ARTICLE

pubs.acs.org/JCTC

# RI-MP2 and MPWB1K Study of $\pi$−Anion−$\pi'$ Complexes: MPWB1K Performance and Some Additivity Aspects

Carolina Garau,[†] Antonio Frontera,*[,†] David Quiñonero,[†] Nino Russo,*[,‡] and Pere M. Deyà[†]

[†]Department de Química, Universitat de les Illes Balears, 07122 Palma de Mallorca, Spain

[‡]Department di Chimica, Università della Calabria, 87036 Arcavacata di Rende (CS), Italy

Supporting Information

**ABSTRACT:** Several sandwich complexes of hexafluorobenzene, trifluorobenzene, *s*-triazine, and trifluoro-*s*-triazine with halides, nitrate, and carbonate anions have been optimized at the RI-MP2/6-31++G** (full and frozen core), B3LYP/6-31++G**, and MPWB1K/6-31++G** levels of theory. All possible combinations of the $\pi$-systems and anions (to generate the sandwich $\pi$−anion−$\pi'$ complexes) have been computed and analyzed using the aforementioned levels of theory. This allows us to evaluate the reliability and the performance of the MPWB1K functional to compute the binding energies of the anion−$\pi$ complexes and to analyze the additivity of the interaction in $\pi$−anion−$\pi'$ complexes where the aromatic rings are of different nature ($\pi$-acidity). We have also explored the Cambridge Structural Database and several interesting X-ray structures that support the theoretical calculations that have been found.

## 1. INTRODUCTION

Noncovalent interactions play a key role in many areas of modern chemistry, especially in the fields of supramolecular chemistry and molecular recognition.[1] Interactions involving aromatic rings are important binding forces in both chemical and biological systems, and they have been recently reviewed.[2] Among them, the favorable interaction of anions with $\pi$-acidic rings, namely anion−$\pi$ interaction,[3] has been extensively studied theoretically.[4] Moreover, the importance of this interaction has been corroborated by a great deal of experimental work. For instance, a new family of anion receptors based on anion−$\pi$ interactions has emerged.[5] In addition, the design and synthesis of highly selective anion channels[6] represents a very significant progress in this nascent field of supramolecular chemistry. In addition, the anion−$\pi$ interaction has been observed in several biological systems. For instance, it participates in the inhibition of the enzyme urate oxidase by cyanide[7] or the enzymatic chlorination of tryptophan by PrnA flavin-dependent halogenase.[8] There are several excellent reviews[9] that describe different aspects of the anion−$\pi$ interaction. From the physicochemical point of view, the anion−$\pi$ interaction is dominated by electrostatic and anion-induced polarization forces.[3] The strength of the electrostatic component depends upon the value of the quadrupole moment of the arene. The anion-induced polarization term correlates with the molecular polarizability ($\alpha_{||}$) of the aromatic compound.[10]

This manuscript is devoted to the study of three different topics of the anion−$\pi$ interaction. First, we report a computational study where we analyze the geometrical and energetic features of anion−$\pi$ complexes at several levels of theory, including ab initio methods (MP2(FC), RI-MP2(FC), and RI-MP2(full)) and density functional theory (DFT) methods (B3LYP and MPWB1K). We study the performance of the MPWB1K[11] method to reproduce the MP2 results in comparison with the more popular B3LYP. It is well-known that DFT, especially with hybrid functionals, allows predicting accurately hydrogen-bonding interactions. However in case of $\pi$−$\pi$ stacking interactions, DFT fails completely,[12] and the use of DFT-D (empirical London dispersion) is required.[13] However this method is less accurate than other functionals in the case of hydrogen-bonded systems. More recently, Truhlar and Zhao[11] developed the MPWB1K functional and demonstrated that it gives good results for both hydrogen-bonding and stacking interactions. Moreover, Dkhissi and Blossey[14] have confirmed the ability of this functional to describe stacking and hydrogen-bonding interactions of nucleic acid bases. They have further demonstrated that the medium basis set (6-31+G**) is sufficient to predict accurately the stacking interactions and, consequently, DFT/MPWB1K is very promising for studies of larger biomolecules (DNA/RNA bases, proteins, etc.).

Since the credibility of the MPWB1K has not been evaluated for anion−$\pi$ interactions, our aim here is to demonstrate that this functional gives results that are comparable to higher level ab initio methods. On the other hand, a previous study has demonstrated that the anion−$\pi$ interaction is approximately additive in a reduced number of ternary $\pi$−anion−$\pi$ complexes where both $\pi$-systems are equal.[15] Furthermore, the additivity of this interaction has been recently studied using a totally different approximation.[16] That is, depending on the number of double bonds and the number of fluorine substituents, the additivity in several complexes of fluorine-substituted ethyne, ethene, butadiene, cyclobutadiene, fulvene, benzene, and [*n*]radialenes ($n$ = 3−5) has been analyzed. However in the second part of this work, we have studied an unexplored aspect of the additivity of the anion−$\pi$ interaction. That is, we have combined four aromatic rings and five anions (see Figure 1), in order to have a large representation of $\pi$−anion−$\pi'$ complexes and with the purpose to study if the interaction is additive in these complexes

**Received:** June 14, 2011
**Published:** August 07, 2011

where the aromatic rings are different using RI-MP2 and MPWB1K methods. In the third part, we have explored the Cambridge Structural Database (CSD),[17] and we have found experimental evidence of the existence of $\pi$−anion−$\pi$ assemblies in X-ray structures that have a strong influence in the crystal packing.

## 2. THEORETICAL METHODS

The geometry of all binary complexes included in this study was fully optimized at the MP2(FC)/6-31++G**, RI-MP2(FC)/6-31++G**, RI-MP2(full)/6-31++G**, MPWB1K/6-31++G**, and B3LYP/6-31++G** level of theory using the Gaussian 03[18] and TURBOMOLE version 5.10.[19] See Supporting Information for Cartesian coordinates of RI-MP2(FC)/6-31++G** and MPWB1K/6-31++G** optimized structures. The RI-MP2 method[20,21] applied to the study of cation−$\pi$ and anion−$\pi$ interactions (among others) is considerably faster than the MP2 method, and the interaction energies and equilibrium distances are almost identical for both methods.[22,23] For the ternary complexes, the optimizations and binding energy calculations were performed only at the RI-MP2(FC)/6-31++G** and MPWB1K/6-31++G** levels of theory. The binding energy was calculated with correction for the basis set superposition error (BSSE) using the Boys−Bernardi counterpoise technique.[24]

The topological analysis of the electron charge density performed for the complexes was determined using Bader's theory of "atoms-in-molecules" (AIM).[25] The electronic density analysis was performed using the AIM2000 program[26] at the RI-MP2-(FC)/6-31++G** level of theory. All complexes are stationary points apart from the fluoride complexes, where the global minimum corresponds to the nucleophilic attack of the fluoride to one carbon atom of the aromatic ring.

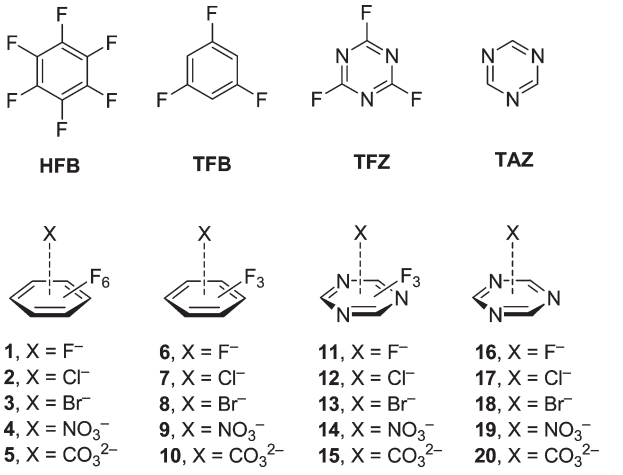


**Figure 1.** Aromatic rings used in this work and anion−$\pi$ complexes **1**−**20**.

## 3. RESULTS AND DISCUSSION

**3.1. Preliminary Calculations.** Table 1 reports the interaction energies and equilibrium distances of binary anion−$\pi$ complexes **1**−**20** at several levels of theory (see Figure 1), which have been computed using both ab initio (MP2(FC), RI-MP2(full), and RI-MP2(FC)) and DFT (MPWB1K and B3LYP) methods and the 6-31++G** basis set. In agreement with previous reports, the ab initio MP2 methods give very similar results, indicating that the frozen core and/or the resolution of the identity (RI) approximations, that significantly reduce the computational time

**Table 1. Interaction Energies Using Several Methods and the 6-31++G** Basis Set With the BSSE Correction ($E_{BSSE}$, kcal/mol) and Equilibrium Distances from the Anion to the Ring Centroid ($R_e$, Å) for Complexes 1−20[a]**

| complex | $E_{BSSE}^{MP2(FC)}$ | $R_e^{MP2(FC)}$ | $E_{BSSE}^{RI\text{-}MP2(full)}$ | $R_e^{RI\text{-}MP2(full)}$ | $E_{BSSE}^{RI\text{-}MP2(FC)}$ | $R_e^{RI\text{-}MP2(FC)}$ | $E_{BSSE}^{MPWB1K}$ | $E_e^{MPWB1K}$ | $E_{BSSE}^{B3LYP}$ | $E_e^{B3LYP}$ |
|---|---|---|---|---|---|---|---|---|---|---|
| **1** (**HFB**−$F^-$) | −18.31 | 2.570 | −18.80 | 2.566 | −18.79 | 2.566 | −19.74 | 2.624 | −17.48 | 2.656 |
| **2** (**HFB**−$Cl^-$) | −12.88 | 3.148 | −13.10 | 3.154 | −12.91 | 3.154 | −12.99 | 3.297 | −10.96 | 3.310 |
| **3** (**HFB**−$Br^-$) | −12.11 | 3.201 | −12.70 | 3.282 | −12.58 | 3.301 | −11.92 | 3.412 | −9.40 | 3.367 |
| **4** (**HFB**−$NO_3^-$) | −12.65 | 2.917 | −12.70 | 2.927 | −12.80 | 2.931 | −10.82 | 2.985 | −8.40 | 2.911 |
| **5** (**HFB**−$CO_3^{2-}$) | −33.07 | 2.720 | −32.10 | 2.750 | −33.01 | 2.744 | −32.09 | 2.755 | −28.37 | 2.880 |
| **6** (**TFB**−$F^-$) | −7.77 | 2.748 | −7.70 | 2.755 | −7.70 | 2.758 | −7.65 | 2.995 | −6.62 | 2.854 |
| **7** (**TFB**−$Cl^-$) | −4.79 | 3.323 | −4.81 | 3.336 | −4.82 | 3.341 | −4.59 (−4.77) | 3.662 (3.656) | −3.31 (−3.39) | 3.626 (2.569) |
| **8** (**TFB**−$Br^-$) | −4.39 | 3.359 | −4.94 | 3.468 | −4.97 | 3.487 | −3.72 | 3.422 | −2.09 | 3.640 |
| **9** (**TFB**−$NO_3^-$) | −5.62 | 3.471 | −5.72 | 3.043 | −5.71 | 3.043 | −4.07 (−4.39) | 3.043 (3.041) | −2.59 (−2.50) | 3.473 (3.421) |
| **10** (**TFB**−$CO_3^{2-}$) | −17.33 | 2.814 | −17.32 | 2.854 | −17.34 | 2.856 | −16.47 | 2.853 | −10.05 | 3.019 |
| **11** (**TFZ**−$F^-$) | −24.23 | 2.390 | −24.32 | 2.385 | −22.23 | 2.385 | −26.30 | 2.327 | −23.01 | 2.416 |
| **12** (**TFZ**−$Cl^-$) | −14.98 | 3.009 | −15.05 | 3.008 | −15.05 | 3.006 | −15.63 (−15.69) | 3.057 (3.054) | −13.00(−13.14) | 3.155 (3.150) |
| **13** (**TFZ**−$Br^-$) | −14.00 | 3.137 | −14.19 | 3.176 | −14.11 | 3.157 | −13.72 | 3.156 | −10.89 | 3.267 |
| **14** (**TFZ**−$NO_3^-$) | −13.01 | 2.805 | −13.04 | 2.814 | −13.06 | 2.816 | −12.21 (−12.32) | 2.830 (2.868) | −8.89 (−8.93) | 3.047 (3.063) |
| **15** (**TFZ**−$CO_3^{2-}$) | −36.94 | 2.505 | −36.95 | 2.520 | −37.95 | 2.520 | −40.21 | 2.508 | −35.30 | 2.602 |
| **16** (**TAZ**−$F^-$) | −9.70 | 2.592 | −9.76 | 2.584 | −9.74 | 2.582 | −11.02 | 2.625 | −8.92 | 2.659 |
| **17** (**TAZ**−$Cl^-$) | −5.22 | 3.223 | −5.27 | 3.220 | −5.24 | 3.219 | −5.57 | 3.475 | −4.01 | 3.475 |
| **18** (**TAZ**−$Br^-$) | −5.01 | 3.339 | −5.05 | 3.338 | −5.22 | 3.402 | −5.23 | 3.462 | −2.99 | 3.582 |
| **19** (**TAZ**−$NO_3^-$) | −5.34 | 3.003 | −5.37 | 3.007 | −5.36 | 3.009 | −4.21 | 3.016 | −2.59 | 3.318 |
| **20** (**TAZ**−$CO_3^{2-}$) | −16.85 | 2.751 | −16.90 | 2.756 | −16.90 | 2.758 | −19.23 | 2.750 | −12.18 | 2.859 |
| rmsd | – | – | 0.31 | 0.102 | 0.54 | 0.104 | 1.323 | 0.162 | 3.107 | 0.181 |

[a] The computed values using the 6-311++G** basis set are indicated in parentheses. The root-mean-square deviation (rmsd) for the different levels with respect to MP2(FC) results is also shown.

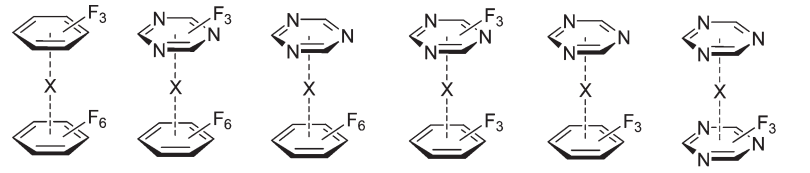

**21**, X = $F^-$ **26**, X = $F^-$ **31**, X = $F^-$ **36**, X = $F^-$ **41**, X = $F^-$ **46**, X = $F^-$
**22**, X = $Cl^-$ **27**, X = $Cl^-$ **32**, X = $Cl^-$ **37**, X = $Cl^-$ **42**, X = $Cl^-$ **47**, X = $Cl^-$
**23**, X = $Br^-$ **28**, X = $Br^-$ **33**, X = $Br^-$ **38**, X = $Br^-$ **43**, X = $Br^-$ **48**, X = $Br^-$
**24**, X = $NO_3^-$ **29**, X = $NO_3^-$ **34**, X = $NO_3^-$ **39**, X = $NO_3^-$ **44**, X = $NO_3^-$ **49**, X = $NO_3^-$
**25**, X = $CO_3^{2-}$ **30**, X = $CO_3^{2-}$ **35**, X = $CO_3^{2-}$ **40**, X = $CO_3^{2-}$ **45**, X = $CO_3^{2-}$ **50**, X = $CO_3^{2-}$

**Figure 2.** Schematic representation of $\pi$−anion−$\pi'$ complexes **21**−**50**.

of calculation, are fully applicable in these systems. A more detailed analysis of Table 1 shows that when comparing the results obtained using RI-MP2(FC) with those obtained using MP2(FC), the largest difference is found in complex **8** (**TFB**−$Br^-$), which is overestimated in 0.6 kcal/mol using the RI approximation. This provokes the bromide complex to become more favorable than the chloride complex, in spite of having a larger equilibrium distance. A similar overestimation (0.5 kcal/mol) is observed in **HFB**−$Cl^-$ and **HFB**−$Br^-$ complexes, although in this case, the chloride complex is more favorable. Moreover, the differences between the interaction energies computed at the RI-MP2(full) and RI-MP2(FC) are also small, being the largest difference 2.1 kcal/mol in the **TFZ**−$F^-$ complex (**11**). The equilibrium distances are almost equivalent for both methods; the maximum difference is 0.06 Å in complex **TAZ**−$Br^-$ (**18**). In spite of these small differences, the utilization of the RI-MP2(FC) method is convenient, since it gives almost identical interaction energies and equilibrium distances with a significantly reduced computational cost.

In terms of energetic and geometric results gathered in Table 1, a good performance of the MPWB1K method is observed since they are comparable to MP2 results. In addition, the MPWB1K method gives much better results than the more popular B3LYP method. In general the B3LYP method underestimates the interaction energies with respect to MP2 results. For instance, the interaction energy of complex **TFB**−$CO_3^{2-}$ at the B3LYP/6-31++G** differs in ∼6 kcal/mol with respect to the other levels of theory. In addition the interaction energies obtained using the B3LYP functional are between 2 and 4 kcal/mol less favorable than the MP2 ones for the rest of the complexes. The equilibrium distances are larger using the DFT than the MP2 methods. For the MPWB1K functional, the largest differences are found in complexes **TAZ**−$Cl^-$ and **TFB**−$Cl^-$ (around 0.3 Å). We have included in Table 1 the root-mean-square deviation (rmsd) between the reference method (MP2(FC)) and the other computational levels. The rmsd values for both RI-MP2 levels are very small for both energies and distances. In addition, the rmsd values obtained for the DFT calculations clearly demonstrate that the MPWB1K method is more reliable than the B3LYP method to study these complexes. Finally, for some complexes (using both MPWB1K and B3LYP functionals), we have also obtained the geometries and energies using the more flexible 6-311++G** basis set (values in parentheses, see Table 1). The geometric and energetic results are almost equivalent, indicating that the 6-31++G** basis set is of sufficient quality to perform this study.

**3.2. Ternary $\pi$−anion−$\pi'$ Complexes.** Once demonstrated in the previous section of the manuscript that the RI-MP2(FC) and MPWB1K methods give reliable and comparable results, we have studied the additivity of the anion−$\pi$ interaction in $\pi$−anion−$\pi'$ complexes using the four aromatic rings used so far (see Figure 1). Two of them (**HFB** and **TFZ**) are strongly $\pi$-acidic (large and positive quadrupole moment), therefore, in their complexes, the interaction will be dominated by both electrostatic and ion-induced polarization effects.[10] The other two aromatic rings (**TFB** and **TAZ**) have negligible quadrupole moments, and the interaction will be dominated only by polarization effects.[27,28] The additivity of the interaction has been analyzed in the ternary $\pi$−anion−$\pi'$ complexes using all possible combinations of **HFB**, **TFB**, **TFZ**, and **TAZ** and the five anions considered in this work ($F^-$, $Cl^-$, $Br^-$, $NO_3^-$, and $CO_3^{2-}$). As a result, we have optimized the complexes **21**−**50** shown in Figure 2 at both RI-MP2(FC)/6-31++G** and MPWB1K/6-31++G** levels of theory.

The energetic and geometric results are summarized in Table 2. In all cases the interaction energies are large and negative, indicating a very favorable interaction. As expected complexes **26**−**30** are more favorable than the rest because both aromatic rings (**HFB** and **TFZ**) present large and positive values of quadrupole moment ($Q_{zz}$ = 9.50 and 8.23 B, respectively). The contrary is observed in complexes **41**−**45** because in this case both aromatic rings (**TFB** and **TAZ**) have negligible values of quadrupole moment ($Q_{zz}$ = 0.19 and 0.99 B, respectively), and the interaction is dominated only by ion-induced polarization effects. For the rest of complexes, where one aromatic ring is electron-deficient ($Q_{zz}$ > 8 B) and the other is neutral ($Q_{zz} \approx 0$ B), the interaction energies are comparable for each series of anions. Therefore the interaction energies exhibit a clear trend depending on the $\pi$-acidity of the rings. For instance, for $F^-$ the interaction energy varies from −39.9 kcal/mol in strong $\pi$-acidic rings to around −28 kcal/mol in hybrid complexes that combine high and low $\pi$-acidic rings and finally to −16 kcal/mol in weak $\pi$-acidic rings. Likewise, the interaction for $Cl^-$, $Br^-$, and $NO_3^-$ varies from around −25 to −18 and to −10 kcal/mol for the same groups, suggesting a qualitative relationship with the $\pi$-acidic nature of the ring.

In Table 2 we also summarize the "ideal" interaction energy ($E_{ideal}$) that is obtained by summing the interaction energies of the two related binary complexes (see Table 1). For instance in ternary complex **21** (**HFB**−$F^-$−**TFB**), the $E_{ideal}$ is the sum of the interaction energies of binary complexes **1** (**HFB**−$F^-$) and **6** (**TFB**−$F^-$). The $E_{ideal}$ can be understood as the expected interaction energy of the ternary complex, considering the interaction is totally additive. From the results reported in Table 2, it can be observed that the difference between the $E_{ideal}$ and the $E_{BSSE}$ ($\Delta E_{ideal}$) is smaller for the ab initio than for the DFT method. As a matter of fact $\Delta E_{ideal}$ is smaller than

Table 2. Interaction Energies (in kcal/mol) with the BSSE Correction for $\pi-$Anion$-\pi'$ Complexes 21−50 at RI-MP2(FC)/6-31++G** and MPWB1K/6-31++G** Levels of Theory[a]

| $\pi-$anion$-\pi'$ complex | $E_{BSSE}^{RI\text{-}MP2}$ | $E_{ideal}^{RI\text{-}MP2}$ | $\Delta E_{ideal}^{RI\text{-}MP2}$ | $R_{\pi-anion}$ | $R_{anion-\pi'}$ | $E_{BSSE}^{MPWB1K}$ | $E_{ideal}^{MPWB1K}$ | $\Delta E_{ideal}^{MPWB1K}$ | $R_{\pi-anion}$ | $R_{anion-\pi'}$ |
|---|---|---|---|---|---|---|---|---|---|---|
| **HFB**−$F^-$−**TFB (21)** | −25.01 | −26.50 | −1.49 | 2.539 | 2.704 | −25.82 | −27.38 | −1.56 | 2.631 | 2.683 |
| **HFB**−$Cl^-$−**TFB (22)** | −17.68 | −17.73 | −0.05 | 3.132 | 3.330 | −17.01 | −17.59 | −0.58 | 3.252 | 3.306 |
| **HFB**−$Br^-$−**TFB (23)** | −17.28 | −17.56 | −0.27 | 3.273 | 3.446 | −14.79 | −15.64 | −0.86 | 3.324 | 3.412 |
| **HFB**−$NO_3^-$−**TFB (24)** | −17.77 | −18.51 | −0.74 | 2.917 | 3.020 | −13.99 | −14.89 | −0.90 | 3.023 | 3.046 |
| **HFB**−$CO_3^{2-}$−**TFB (25)** | −47.42 | −50.34 | −2.92 | 2.742 | 2.886 | −44.88 | −48.57 | −3.68 | 2.766 | 3.020 |
| **HFB**−$F^-$−**TFZ (26)** | −39.94 | −41.02 | −1.08 | 2.374 | 2.617 | −41.86 | −46.04 | −4.17 | 2.642 | 2.368 |
| **HFB**−$Cl^-$−**TFZ (27)** | −26.65 | −27.96 | −1.31 | 2.974 | 3.103 | −27.20 | −28.62 | −1.42 | 3.253 | 3.063 |
| **HFB**−$Br^-$−**TFZ (28)** | −25.61 | −26.69 | −1.08 | 3.182 | 3.277 | −24.27 | −25.64 | −1.38 | 3.308 | 3.144 |
| **HFB**−$NO_3^-$−**TFZ (29)** | −24.07 | −25.85 | −1.78 | 2.815 | 2.919 | −20.99 | −23.03 | −2.04 | 3.017 | 2.890 |
| **HFB**−$CO_3^{2-}$−**TFZ (30)** | −63.53 | −70.06 | −6.53 | 2.567 | 2.765 | −63.46 | −72.31 | −8.85 | 2.778 | 2.563 |
| **HFB**−$F^-$−**TAZ (31)** | −27.14 | −28.53 | −1.39 | 2.552 | 2.570 | −28.54 | −30.75 | −2.22 | 2.633 | 2.570 |
| **HFB**−$Cl^-$−**TAZ (32)** | −18.09 | −18.16 | −0.06 | 3.135 | 3.220 | −17.92 | −18.56 | −0.64 | 3.132 | 3.216 |
| **HFB**−$Br^-$−**TAZ (33)** | −17.57 | −17.80 | −0.24 | 3.279 | 3.380 | −15.36 | −17.15 | −1.79 | 3.262 | 3.376 |
| **HFB**−$NO_3^-$−**TAZ (34)** | −17.45 | −18.16 | −0.71 | 2.920 | 3.006 | −14.14 | −15.03 | −0.89 | 3.020 | 3.038 |
| **HFB**−$CO_3^{2-}$−**TAZ (35)** | −46.92 | −49.91 | −2.99 | 2.749 | 2.794 | −46.64 | −51.32 | −4.68 | 2.769 | 2.787 |
| **TFB**−$F^-$−**TFZ (36)** | −30.41 | −29.93 | 0.48 | 2.724 | 2.378 | −32.34 | −33.95 | −1.60 | 2.692 | 2.343 |
| **TFB**−$Cl^-$−**TFZ (37)** | −19.56 | −19.87 | −0.31 | 3.312 | 3.014 | −19.68 (−21.80) | −20.22 (−20.46) | −0.55 (1.34) | 3.302 (3.299) | 3.059 (3.063) |
| **TFB**−$Br^-$−**TFZ (38)** | −18.72 | −19.08 | −0.36 | 3.462 | 3.183 | −16.79 | −17.45 | −0.66 | 3.390 | 3.149 |
| **TFB**−$NO_3^-$−**TFZ (39)** | −18.07 | −18.77 | −0.70 | 3.023 | 2.803 | −14.94 (−15.30) | −16.28 (−16.71) | −1.34 (−1.41) | 3.037 (3.031) | 2.867 (2.863) |
| **TFB**−$CO_3^{2-}$−**TFZ (40)** | −50.55 | −54.39 | −3.84 | 2.888 | 2.541 | −51.26 | −56.69 | −5.43 | 3.017 | 2.525 |
| **TFB**−$F^-$−**TAZ (41)** | −16.93 | −17.44 | −0.51 | 2.750 | 2.583 | −17.87 | −18.66 | −0.79 | 2.683 | 2.570 |
| **TFB**−$Cl^-$−**TAZ (42)** | −10.13 | −10.06 | 0.06 | 3.328 | 3.223 | −10.26 | −10.16 | 0.10 | 3.319 | 3.398 |
| **TFB**−$Br^-$−**TAZ (43)** | −10.32 | −10.20 | 0.12 | 3.531 | 3.432 | −8.49 | −8.95 | −0.46 | 3.413 | 3.476 |
| **TFB**−$NO_3^-$−**TAZ (44)** | −10.96 | −11.07 | −0.11 | 3.027 | 2.995 | −7.80 | −8.27 | −0.47 | 3.041 | 3.038 |
| **TFB**−$CO_3^{2-}$−**TAZ (45)** | −32.54 | −34.24 | −1.70 | 2.868 | 2.773 | −32.57 | −35.70 | −3.14 | 3.009 | 2.778 |
| **TFZ**−$F^-$−**TAZ (46)** | −32.32 | −31.97 | 0.35 | 2.382 | 2.577 | −35.01 | −37.32 | −2.31 | 2.366 | 2.572 |
| **TFZ**−$Cl^-$−**TAZ (47)** | −19.96 | −20.29 | −0.33 | 3.008 | 3.220 | −20.85 | −21.20 | −0.34 | 3.063 | 3.387 |
| **TFZ**−$Br^-$−**TAZ (48)** | −18.93 | −19.33 | −0.40 | 3.186 | 3.382 | −18.07 | −18.95 | −0.88 | 3.157 | 3.467 |
| **TFZ**−$NO_3^-$−**TAZ (49)** | −16.97 | −18.42 | −1.45 | 2.809 | 3.004 | −15.47 | −16.41 | −0.94 | 2.831 | 3.025 |
| **TFZ**−$CO_3^{2-}$−**TAZ (50)** | −49.85 | −53.96 | −4.10 | 2.547 | 2.811 | −52.47 | −59.45 | −6.98 | 2.540 | 2.797 |
| **rmsd** | - | - | - | - | - | 1.93 | 2.48 | 1.27 | 0.111 | 0.086 |

[a] The ideal interaction energy (sum of the energies of the corresponding binary complexes, $E_{ideal}$) and the difference between this energy and the interaction energy ($\Delta E_{ideal}$) are also shown. The computed values using the 6-311++G** basis set are indicated in parentheses. The rmsd for the different levels with respect to MP2(FC) results is also shown.

2 kcal/mol for all complexes apart from $CO_3^{2-}$ complexes at the RI-MP2/6-31++G** level of theory. Therefore the interaction energy is approximately additive for all monoanionic complexes. For carbonate dianion, the $\Delta E_{ideal}$ values are greater than for the rest of complexes, ranging from −1.7 to −6.5 kcal/mol. However it should be remarked that the interaction energy in these complexes is very large, and therefore the difference between the "ideal" and "real" interaction energies increases. In addition the two negative charges of the carbonate ion may promote a larger polarization in the sandwich complex than in the two binary anion$-\pi$ complexes. In addition, in almost all complexes, the $\Delta E_{ideal}$ energies are negative, which means that the interaction energy is always less favorable than expected from the sum of the interaction energies of the binary complexes. Regarding the equilibrium distances, they are mostly unaffected by the presence of an additional anion$-\pi$ interaction. As an example, in all ternary complexes of chloride, which are represented in Figure 3, the equilibrium distances are almost equivalent with respect to the related binary complexes. For the rest of the complexes, the largest variation is found in complex **TFB**−$Br^-$−**TAZ (43)**, where the $\pi-$anion distance increases in 0.063 Å and the anion$-\pi'$ distance increases in 0.094 Å. Finally, the performance of the DFT method should be emphasized since it is able to reproduce the interaction energies of the ternary complexes computed at the RI-MP2(FC)/6-31++G** level of theory. The agreement of MPWB1K and RI-MP2(FC) methods is illustrated in Figure 4 and the rmsd values provided in Table 2. For two complexes, we have also validated the utilization of the 6-31++G** basis set by computing the geometries and the energies at the MPWB1K/6-311++G** level of theory and obtaining very similar results (values in parentheses in Table 2).

To further confirm the additivity of the anion$-\pi$ interaction in these systems, we have used the Bader's theory of atoms in molecules (AIM), which provides an unambiguous definition of chemical bonding,[29] using the MP2(FC)/6-31++G** wave function. The AIM theory has been successfully used to characterize anion$-\pi$ interactions and to analyze nonadditivity effects.[16] The distribution of critical points in several representative complexes is shown in Figure 5. For the anion$-\pi$ complex **12** (**TFZ**−$Cl^-$), the exploration of the CPs revealed the presence of three bond

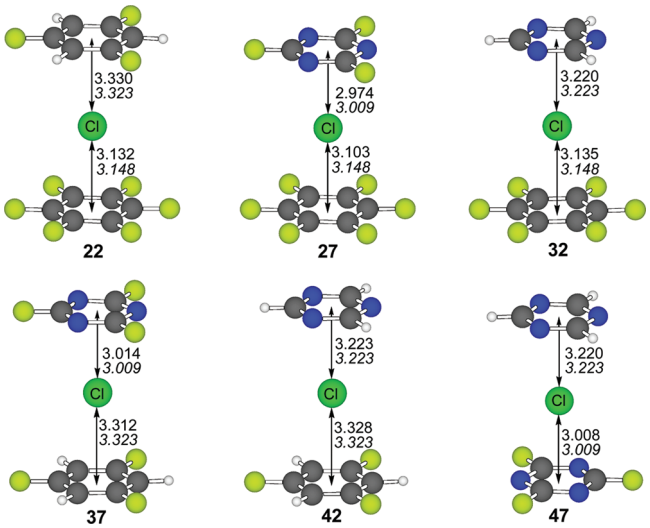


**Figure 3.** RI-MP2(FC)/6-31++G** optimized structures of $\pi-Cl^{-}-\pi'$ complexes. Distances (in Å) in italics correspond to the binary anion$-\pi$ complexes.

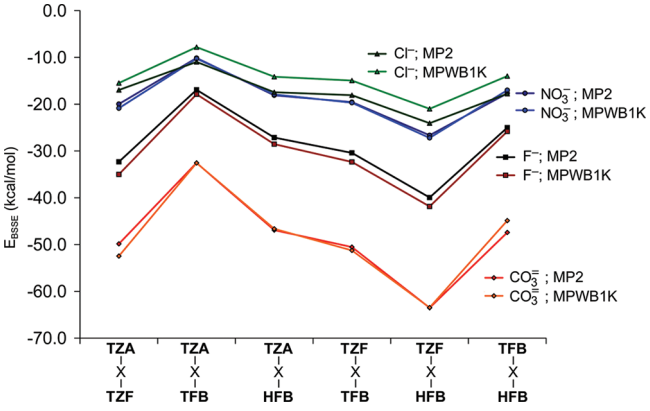


**Figure 4.** Plot of the interaction energies of all series of $\pi-X-\pi'$ complexes (X = $F^{-}$, $Cl^{-}$, $NO_3^{-}$, and $CO_3^{2-}$) at two levels of theory. The bromide complexes have been omitted for clarity.

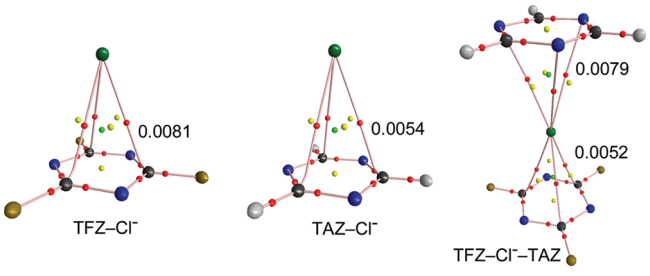


**Figure 5.** Schematic representation of the CPs obtained for complexes **12** (TFZ$-Cl^{-}$), **17** (TAZ$-Cl^{-}$), and **47** (TFZ$-Cl^{-}-$TAZ). Bond CPs are represented in red, ring CPs in yellow, and cage CPs in green. The values of $\rho$ at the cage CPs are in atomic units.

and three ring CPs that connect the anion with the carbon and nitrogen atoms of the arene, respectively. The interaction is further described by the presence of a cage CP that it is located along the main symmetry axis (see Figure 5). The distribution of the CPs for complex **17** (**TAZ**$-Cl^{-}$) is identical. In the

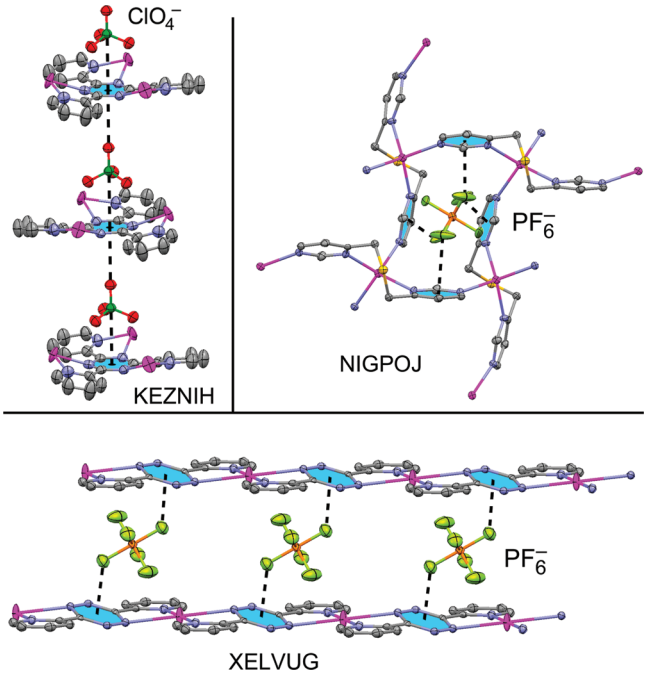


**Figure 6.** Selected fragments of the X-ray crystal structures of KEZNIH, NIGPOJ and XELVUG.

$\pi-$anion$-\pi'$ complex **47** (**TFZ**$-Cl^{-}-$**TAZ**) the exploration of the CPs revealed the same number and distribution than the binary complexes. A common feature of the complexes is the presence of a cage CP linking the anion with the center of the ring, as is common in the anion$-\pi$ complexes.[4] As a matter of fact, the value of the charge density ($\rho$) at the cage CP has been used as a measure of bond order, and it is related to the strength of the interaction.[4] In Figure 5 we have included the values of $\rho$ at the cage CPs. It can be appreciated that the value of $\rho$ in complex **12** is considerably greater than the one for complex **17**, in agreement with the interaction energies (see Table 1). It is interesting to compare the values of $\rho$ obtained for the ternary complex **47** to those of the binary complexes **12** and **17**. It can be observed that the values of $\rho$ are very similar (see Figure 5), indicating that the bond order of each anion$-\pi$ interaction in the ternary complex does not change with respect to the binary complexes. Consequently, each interaction is not affected by the presence of the second aromatic ring, thus confirming the additivity of the anion$-\pi$ interaction.

**3.4. CSD Study.** The CSD[17] is a convenient and reliable storehouse for geometrical information. The utility of small-molecule crystallography and the CSD in analyzing geometrical parameters and nonbonding interactions is well established.[30] We have explored the CSD searching crystallographic fragments where $\pi-$anion$-\pi$ assemblies are present in the solid state. We show in Figure 6 three selected examples (CSD reference codes: KEZNIH,[31] NIGPOJ,[32] and XELVUG)[33] that we have retrieved from the database where the $\pi-$anion$-\pi$ binding motif is very relevant and crucial in the crystal packing. The KEZNIH structure was published by Zhou et al.[31] as a part of a very interesting manuscript where the authors report the self-assembly of Ag(I) coordination networks directed by anion$-\pi$ interactions. In their study of Ag(I) metal complexes with 2,4,6-tri(2-pyridyl)-1,3,5-triazine (tpt), they found that polyatomic anions ($ClO_4^{-}$, $BF_4^{-}$, and $PF_6^{-}$) directed the self-assembly of Ag-tpt

coordination polymers through infinite $\pi$−anion−$\pi$ interactions, as can be observed in the X-ray structure shown in Figure 6, where the anions interact with the central triazine ring of the tpt ligands in the X-ray crystal structure. Notably, the same binding motif is found in the other two X-ray structures published by Zhou et al. using $BF_4^-$ and $PF_6^-$ as counterions and the same ligand. In fact, in all three structures, the anions are located on the $C_3$-axis above and below the central triazine rings of the tpt ligands, as it is observed in KEZNIH. The XELVUG structure was reported by Dunbar and co-workers in their investigation on the role of anion−$\pi$ interactions in the assembly of Ag(I) complexes using the 3,6-bis(2-pyridyl)-1,2,4,5-tetrazine (bptz) ligand.[33] This work was the first example of a comprehensive investigation of anion−$\pi$ interactions as controlling elements in self-assembly reactions. They reported the formation of complexes of different structural types depending on the experimental conditions and the anion used. Interestingly the reaction of Ag(I) and bptz in a 1:1 ratio in the presence of $PF_6^-$ ions afforded a polymer, as indicated by the single-crystal X-ray structural determination (Figure 6, bottom). Anion−$\pi$ interactions are a major factor in stabilizing the structural motif where the anion is sandwiched between two central *s*-tetrazine rings of the ligands. Finally, NIGPOJ structure was published by Black et al.,[32] and it consists in a coordination polymer formed from Ag(I) ions and bis(4-pyrimidylmethyl)sulphide. It has the ability to encapsulate $PF_6^-$ anion via a uniform mode of $\pi$−anion−$\pi$ binding. The combination of this ligand with silver salts of other anions like $BF_4^-$ and $ClO_4^-$ in a 1:1 molar ratio gives isomorphous complexes. Anions embedded in the cavities formed by this open network are held in place by four complementary $\pi$−anion−$\pi$ sandwich interactions with two pyrimidine rings (see Figure 6). These three important investigations provide strong experimental evidence for the usefulness of $\pi$-acidic rings in the design of anion receptors coordinated to transition-metal ions (that increase the $\pi$-acidity of the ring), which are bound to their counterions via multiple $\pi$−anion−$\pi$ interactions, demonstrating the potential use of this binding motif in a structurally directing role.

## 4. CONCLUSION

The results derived from this study reveal that the interaction energies and the equilibrium distances of several anion−$\pi$ complexes are well described using the MPWB1K functional. The performance of this method is considerably better than the widely used B3LYP functional in comparison to the ab initio MP2 method. In addition, the ability of the MPWB1K functional to describe the energetic and geometric parameters in $\pi$−anion−$\pi'$ complexes has been demonstrated. Moreover, we have also demonstrated that the interaction is approximately additive in these complexes, especially when the anion is monoanionic. Finally, we have explored the CSD, and we have found several interesting examples where the $\pi$−anion−$\pi$ assemblies are crucial to understand the architecture of the X-ray structure. Therefore, the potential of multiple anion−$\pi$ interactions for the design of novel sensors, hosts, catalysts, and materials is anticipated.

## ■ ASSOCIATED CONTENT

**Ⓢ Supporting Information.** Cartesian coordinates of RI-MP2(FC)/6-31++G** and MPWB1K/6-31++G** optimized structures. This material is available free of charge via the Internet at http://pubs.acs.org.

## ■ AUTHOR INFORMATION

**Corresponding Author**

*E-mail: toni.frontera@uib.es, nrusso@unical.it.

## ■ ACKNOWLEDGMENT

We thank CONSOLIDER−Ingenio 2010 (CSD2010-0065) and the MICINN of Spain (project CTQ2008-00841/BQU, FEDER funds) for financial support. We thank the CESCA for computational facilities. D.Q. thanks the MICINN of Spain for a "Ramón y Cajal" contract.

## ■ REFERENCES

(1) Hunter, C. A.; Sanders, J. K. M. *J. Am. Chem. Soc.* **1990**, *112*, 5525.

(2) (a) Salonen, L. M.; Ellermann, M.; Diederich, F. *Angew. Chem., Int. Ed.* **2011**, *50*, 4808. (b) Meyer, E. A.; Castellano, R. K.; Diederich, F. *Angew. Chem., Int. Ed.* **2003**, *42*, 1210.

(3) (a) Mascal, M.; Armstrong, A.; Bartberger, M. *J. Am. Chem. Soc.* **2002**, *124*, 6274. (b) Alkorta, I.; Rozas, I.; Elguero, J. *J. Am. Chem. Soc.* **2002**, *124*, 8593. (c) Quiñonero, D.; Garau, C.; Rotger, C.; Frontera, A.; Ballester, P.; Costa, A.; Deyà, P. M. *Angew. Chem., Int. Ed.* **2002**, *41*, 3389.

(4) Frontera, A.; Quiñonero, D.; Deyà, P. M. *WIREs: Comput. Mol. Sci.* **2011**, *1*, 440.

(5) (a) Rosokha, Y. S.; Lindeman, S. V.; Rosokha, S. V.; Kochi, J. K. *Angew. Chem., Int. Ed.* **2004**, *43*, 4650. (b) Han, B.; Lu, J. J.; Kochi, J. K. *Cryst. Growth Des.* **2008**, *8*, 1327. (c) de Hoog, P.; Gamez, P.; Mutikainen, H.; Turpeinen, U.; Reedijk, J. *Angew. Chem., Int. Ed.* **2004**, *43*, 5815. (d) Estarellas, C.; Rotger, M. C.; Capó, M.; Quiñonero, D.; Frontera, A.; Costa, A.; Deyà, P. M. *Org. Lett.* **2009**, *11*, 1987. (e) Mascal, M.; Yakovlev, I.; Nikitin, E. B.; Fettinger, J. C. *Angew. Chem., Int. Ed.* **2007**, *46*, 8782. (f) Chifotides, H. T.; Schottel, B. L.; Dunbar, K. R. *Angew. Chem., Int. Ed.* **2010**, *49*, 7202. (g) Campos-Fernandez, C. S.; Schottel, B. L.; Chifotides, H. T.; Bera, J. K.; Bacsa, J.; Koomen, J. M.; Russell, D. H.; Dunbar, K. R. *J. Am. Chem. Soc.* **2005**, *127*, 12909. (h) Berryman, O. B.; Hof, F.; Hynes, M. J.; Johnson, D. W. *Chem. Commun.* **2006**, 506. (i) Berryman, O. B.; Sather, A. C.; Hay, B. P.; Meisner, J. S.; Johnson, D. W. *J. Am. Chem. Soc.* **2008**, *130*, 10895. (j) Gil-Ramirez, G.; Escudero-Adan, E. C.; Benet-Buchholz, J.; Ballester, P. *Angew. Chem., Int. Ed.* **2008**, *47*, 4114.

(6) (a) Mareda, J.; Matile, S. *Chem.—Eur. J.* **2009**, *15*, 28. (b) Gorteau, V.; Bollot, G.; Mareda, J.; Matile, S. *Org. Biomol. Chem.* **2007**, *5*, 3000. (c) Gorteau, V.; Bollot, G.; Mareda, J.; Perez-Velasco, A.; Matile, S. *J. Am. Chem. Soc.* **2006**, *128*, 14788. (d) Gorteau, V.; Julliard, M. D.; Matile, S. *J. Membr. Sci.* **2008**, *321*, 37. (e) Perez-Velasco, A.; Gorteau, V.; Matile, S. *Angew. Chem., Int. Ed.* **2008**, *47*, 921. (f) Dawson, R. E.; Hennig, A.; Weimann, D. P.; Emery, D.; Ravikumar, V.; Montenegro, J.; Takeuchi, T.; Gabutti, S.; Mayor, M.; Mareda, J.; Schalley, C. A.; Matile, S. *Nature Chem.* **2010**, *2*, 533. (g) Sakai, N.; Mareda, J.; Vauthey, E.; Matile, S. *Chem. Commun.* **2010**, *46*, 4225.

(7) Estarellas, C.; Frontera, A.; Quiñonero, D.; Deyà, P. M. *Angew. Chem., Int. Ed.* **2011**, *50*, 415.

(8) Estarellas, C.; Frontera, A.; Quiñonero, D.; Deyà, P. M. *Chem. Asian J.* **2011**in press.

(9) (a) Schottel, B. L.; Chifotides, H. T.; Dunbar, K. R. *Chem. Soc. Rev.* **2008**, *37*, 68. (b) Caltagirone, C.; Gale, P. A. *Chem. Soc. Rev.* **2009**, *38*, 520. (c) Robertazzi, A.; Krull, F.; Knapp, E.-W.; Gamez, P. *CrystEngComm* **2011**, *13*, 3293.

(10) Garau, C.; Frontera, A.; Quiñonero, D.; Ballester, P.; Costa, A.; Deyà, P. M. *ChemPhysChem* **2003**, *4*, 1344.

(11) Zhao, Y.; Truhlar, D. G. *J. Phys. Chem. A* **2004**, *108*, 6908.

(12) Cerny, J.; Hobza, P. *Phys. Chem. Chem. Phys.* **2005**, *7*, 1624.

(13) Elsner, M.; Hobza, P.; Frauenheim, T.; Suhai, S.; Kaxiras, E. *J. Chem. Phys.* **2001**, *114*, 5149.
(14) Dkhissi., A.; Blossey, R. *Chem. Phys. Lett.* **2007**, *439*, 35.
(15) Garau, C.; Quiñonero, D.; Frontera, A.; Ballester, P.; Costa, A.; Deyà, P. M. *J. Phys. Chem. A* **2005**, *109*, 341.
(16) Estarellas, E.; Frontera, A.; Quiñonero, D.; Deyà, P. M. *J. Phys. Chem. A* **2011**, *115*, 7849.
(17) Allen, F. H. *Acta Crystallogr., Sect. B* **2002**, *58*, 380.
(18) Frisch, M. J.; Trucks, G. W.; Schlegel, H. B.; Scuseria, G. E.; Robb, M. A.; Cheeseman, J. R.; Montgomery, J. A., Jr.; Vreven, T.; Kudin, K. N.; Burant, J. C.; Millam, J. M.; Iyengar, S. S.; Tomasi, J.; Barone, V.; Mennucci, B.; Cossi, M.; Scalmani, G.; Rega, N.; Petersson, G. A.; Nakatsuji, H.; Hada, M.; Ehara, M.; Toyota, K.; Fukuda, R.; Hasegawa, J.; Ishida, M.; Nakajima, T.; Honda, Y.; Kitao, O.; Nakai, H.; Klene, M.; Li, X.; Knox, J. E.; Hratchian, H. P.; Cross, J. B.; Bakken, V.; Adamo, C.; Jaramillo, J.; Gomperts, R.; Stratmann, R. E.; Yazyev, O.; Austin, A. J.; Cammi, R.; Pomelli, C.; Ochterski, J. W.; Ayala, P. Y.; Morokuma, K.; Voth, G. A.; Salvador, P.; Dannenberg, J. J.; Zakrzewski, V. G.; Dapprich, S.; Daniels, A. D.; Strain, M. C.; Farkas, O.; Malick, D. K.; Rabuck, A. D.; Raghavachari, K.; Foresman, J. B.; Ortiz, J. V.; Cui, Q.; Baboul, A. G.; Clifford, S.; Cioslowski, J.; Stefanov, B. B.; Liu, G.; Liashenko, A.; Piskorz, P.; Komaromi, I.; Martin, R. L.; Fox, D. J.; Keith, T.; Al-Laham, M. A.; Peng, C. Y.; Nanayakkara, A.; Challacombe, M.; Gill, P. M. W.; Johnson, B.; Chen, W.; Wong, M. W.; Gonzalez, C.; Pople, J. A. *Gaussian 03*, revision C.01; Gaussian, Inc., Wallingford, CT, 2004.
(19) Ahlrichs, R.; Bär, M.; Hacer, M.; Horn, H.; Kömel, C. *Chem. Phys. Lett.* **1989**, *162*, 165.
(20) Feyereisen, M. W.; Fitzgerald, G.; Komornicki, A. *Chem. Phys. Lett.* **1993**, *208*, 359.
(21) Vahtras, O.; Almlof, J.; Feyereisen, M. W. *Chem. Phys. Lett.* **1993**, *213*, 514.
(22) Frontera, A.; Quiñonero, D.; Garau, C.; Ballester, P.; Costa, A.; Deyà, P. M. *J. Phys. Chem. A* **2005**, *109*, 4632.
(23) Quiñonero, D.; Garau, C.; Frontera, A.; Ballester, P.; Costa, A.; Deyà, P. M. *J. Phys. Chem. A* **2006**, *110*, 5144.
(24) Boys, S. B.; Bernardi, F. *Mol. Phys.* **1970**, *19*, 553.
(25) Bader, R. F. W. *Chem. Rev.* **1991**, *91*, 893.
(26) Biegler-König, F; Schönbohm, J.; Bayles, D *J. Comput. Chem.* **2001**, *22*, 545.
(27) Garau, C.; Quiñonero, D.; Frontera, A.; Ballester, P.; Costa, A.; Deyà, P. M. *Org. Lett.* **2003**, *5*, 2227.
(28) Garau, C.; Frontera, A.; Quiñonero, D.; Ballester, P.; Costa, A.; Deyà, P. M. J. *Phys. Chem. A* **2004**, *108*, 9423.
(29) Bader, R. F. W. *J. Phys. Chem. A* **1998**, *102*, 7314.
(30) Nangia, A.; Biradha, K.; Desiraju, G. R. *J. Chem. Soc., Perkin Trans. 2* **1996**, 943.
(31) Zhou, X. P.; Zhang, X. J.; Lin, S. H.; Li, D. *Cryst. Growth Des.* **2007**, *7*, 485.
(32) Black, C. A.; Hanton, L. R.; Spicer, M. D. *Chem. Commun.* **2007**, 3171.
(33) Schottel, B. L.; Chifotides, H. T.; Shatruk, M.; Chouai, A.; Perez, L. M.; Bacsa, J.; Dunbar, K. R. *J. Am. Chem. Soc.* **2006**, *128*, 5895.